Chemistry–A European Journal
Research Article
doi.org/10.1002/chem.202402279
Chemistry Europe
European Chemical Societies Publishing
www.chemeurj.org

Investigating the Catalytic Site of Human 15-Lipoxygenase-1 *via* Marine Natural Products

Ntaniela Spacho[+],[a] Marcello Casertano[+],[b] Concetta Imperatore,[b] Christos Papadopoulos,[a] Marialuisa Menna,*[b] and Nikolaos Eleftheriadis*[a]

Human 15-lipoxygenase-1 (15-LOX-1) is a key enzyme that possesses an important role in (neuro)inflammatory diseases. The pocket of the enzyme plays the role of a chiral catalyst, and therefore chirality could be an important component for the design of effective enzyme inhibitors. To advance our knowledge on this concept, we developed a library of the identified chiral 15-LOX-1 inhibitors and applied cheminformatic tools. Our analysis highlighted specific structural elements, which we integrated them in small molecules, and employed them as "smart" tools to effectively navigate the chemical space of previously unexplored regions. To this purpose, we utilized the marine derived natural product phosphoeleganin (**PE**) among with a small library of synthetic fragment derivatives, including a certain degree of stereochemical diversity. Enzyme inhibition/kinetic and molecular modelling studies has been performed in order to characterize structurally novel PE-based inhibitors, which proved to present a different type of inhibition with low micromolar potency, according to their structural features. We demonstrate that different warheads work as anchor, and either guide specific stereochemistry, or causing a time-depended inhibition. Finally, we prove that the positioning of the chiral substituents or/and the favorable stereochemistry can be crucial, as it can lead from active to completely inactive compounds.

Introduction

Human 15-lipoxygenase-1 (15-LOX-1) is an important enzyme that possesses a regulatory role in inflammatory lung diseases,[1–5] in various CNS diseases,[6–15] as well as in many aspects of human cancer and hematologic malignancies.[16–24] It belongs to lipoxygenase family (5-, 8-, 12- and 15-LOX in mammals), which are enzymes that catalyze the regio- and stereospecific insertion of oxygen into polyunsaturated fatty acids, as arachidonic (AA) or linoleic (LA) acid. This activity leads to the generation of important signaling compounds that regulate several inflammatory diseases.[5,25,26] It has been proposed that 15-LOX-1 is involved both in inflammatory and ferroptosis pathways, displaying a dual biological role.[27–32] Full exploitation of the role of 15-LOX-1 in those complex pathways is not possible without selective small molecules inhibitors that restrain its function. Due to available, but limited, structural information (PDB: 1LOX, 2P0M), most of the known 15-LOX-1 inhibitors have been designed to target the active site of the enzyme, aiming for a competitive inhibition. The 15-LOX-1's active site has a polar entrance but mainly is an extended lipophilic pocket with specific volume, length and geometry, designed to bind particular fatty acids in an exact position with the conservative **Arg403** to play a key role (Figure 1A).[33] The catalytic mechanism includes the substrate binding, its regio-specific peroxidation, and finally the release of a chiral product with a definite stereochemistry. That simply means that the pocket of the enzyme plays the role of a chiral catalyst, and therefore chirality could be an important component for the design of an effective enzyme inhibitor.

Many competitive 15-LOX-1 inhibitors have been developed, with the majority of them containing various privileged scaffolds (Figure 1B). Another big category of identified inhibitors are the phenolic compounds, whose mode of action is based on their antioxidant activity and iron-chelating potential (Figure S1). However, so far very few of the known inhibitors escape from the flat land (aromatic compounds), presenting a chirality preference on the inhibitory potency. Among these, there are our previously developed enantiomerically pure compounds **Eleftheriadis-14 d**[34] (Figure 1C) and **2 b** (Figure 2A).[35] Both these compounds contain a stereogenic center, and it has been demonstrated that their stereochemistry (*S* and *R*, respectively) affect the affinity by a 3-fold difference in potency with respect to the other enantiomer.[34,35] In the same view, other bioactive compounds against 15-LOX, such as phospholipids and amide derivatives of their fatty acids, presenting a chiral or iron chelating component, are also not extensively studied (Figure 1C). It is well known that biological targets can recognize their ligands three-dimensionally (3D), and it is therefore logical to assume that molecules with a greater degree of 3D shape will interact with their targets with

[a] N. Spacho,[+] C. Papadopoulos, N. Eleftheriadis
Department of Chemistry, University of Crete, 70013 Voutes, Heraklion, Greece
E-mail: n.eleftheriadis@uoc.gr
[b] M. Casertano,[+] C. Imperatore, M. Menna
Department of Pharmacy, University of Naples "Federico II", Via D. Montesano 49, 80131 Naples, Italy
E-mail: mlmenna@unina.it
[+] These authors contributed equally to this work.

Supporting information for this article is available on the WWW under https://doi.org/10.1002/chem.202402279

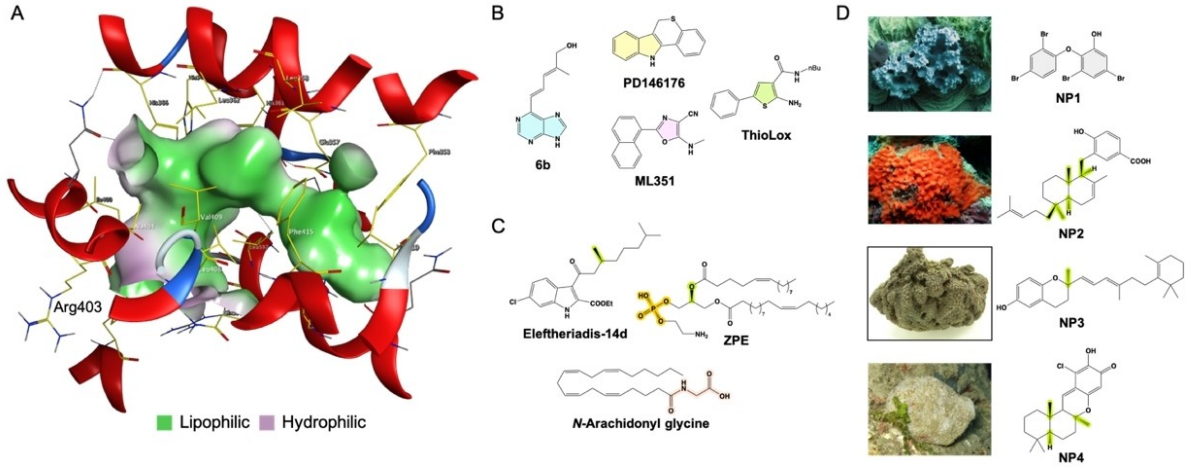

Figure 1. A) The extended lipophilic pocket of the enzyme 15-LOX-1. The lipophilic and hydrophilic parts are represented with green and pink color, respectively. B) Previously identified 15-LOX-1 inhibitors containing various hetero aromatic rings (presented with different colors). C) Previously described 15-LOX-1 bioactive compounds either presenting a chirality preference on the inhibitory potency (Eleftheriadis-14d) or other important structural elements (phosphate group and glycine warhead). D) Previously identified marine natural products as 15-LOX-1 inhibitors.

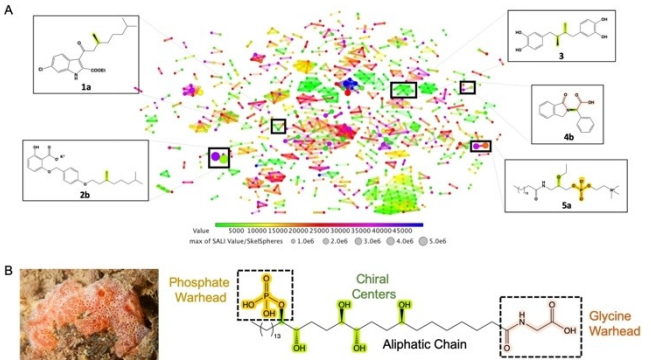

Figure 2. A) The SALI plot of >1600 15-LOX-1 inhibitors (<100 μM potency), containing at least one chiral center, demonstrates the activity gained (or lost) with a relatively small change in structure. The generated similarity view encodes SALI values and activities in marker size and color, respectively. B) The Mediterranean ascidian *Sidnyum elegans* and the structure of PE natural product, highlighting the essential structural elements (green: chiral centers; brown: phosphate group; pink: glycine warhead).

higher affinity and higher levels of specificity.[36] To advance our knowledge on these uncharted concepts and structural features, we need to utilize small molecules with chiral different substituents as "smart" tools in order to effectively navigate the chemical space of previously unexplored regions.

Natural products (NPs) are a great resource for this purpose, due to their high chemical diversity improved through evolutionary selection to effectively interact with biomolecules binding sites. NPs have been widely used in target-based drug discovery due to their favorable structural key properties: 3D structures rich in sp^3 hybridized carbon, often with chiral moieties.[37–39] In addition, NPs may serve as biologically validated starting points for the design of focused libraries that might provide protein ligands with enhanced quality and probability. Especially helpful for this purpose is to employ the Fragment-Based Lead Discovery (FBLD) strategy, in which libraries of fragments (typically MW < 300) that are inspired by already known drugs or candidates are created, aiming for the targeted exploration of the biologically relevant chemical space.

Particularly, over the past half-century, marine NPs are paving the way for chemical and biological novelties.[40] To the extremely rich marine biodiversity, quite different from the terrestrial one, an equally large diversity, extending to both the chemical structures and biological activities of these compounds, is indeed associated. There are examples of natural molecules from the sea that have been tested against the 15-LOX-1 enzyme presenting a good inhibitory activity. The first marine-derived 15-LOX inhibitors discovered were the polybrominated ethers isolated from the sponge *Dysidea* sp. collected in Indo-Pacific Ocean, compound **NP1** (Figure 1D), with an IC_{50} of 15 μM, and its derivatives (compounds **1–4**, Figure S1).[41] Two sesterpenes, (−)-jaspic acid (**NP2**, Figure 1D) and (−)-subersic acid (**5**, Figure S1), were isolated from the sponges *Jaspis splendens* and *Subea sp.*, and identified as potent inhibitors of 15-LOX showing IC_{50} of 1.4 μM and 15 μM, respectively. Bioprospecting of the marine sponge *Psammocinia sp.* afforded the chromarol-derived compounds (**NP3**, Figure 1D; **6–10**, Figure S1) which were revealed as potent and selective inhibitors of human 15-LOX with IC_{50} values ranging from 0.6 to 4.0 μM.[42,43] Finally, 21-chloropuupehenone (**NP4**, Figure 1D; **11**, Figure S1) isolated from *Hyrtios sp.* was found out as potent but nonselective 15-LOX inhibitor with an IC_{50} of 0.83 ± 0.04 μM.[44] However, we can again observe that most of these inhibitors (Figure 1 and S1) have a predominantly planar structure consisting of an aromatic or heteroaromatic portion.

Herein, we utilized a marine NP, phoshoeleganin (**PE**, Figure 2B), together with a pool of PE-based (semi)synthetic fragments obtained by a FBLD approach (Figure S2), as unique chemical tools against the human 15-LOX-1 to investigate the unexplored features of enzyme's active site. This novel molecule was selected based on its good degree of 3D shape, resembling that of the enzyme's natural substrates, and the presence of several stereogenic centers in its acyclic skeleton. Exploration of

the biologically relevant chemical space of **PE** by synthetic means, the structure activity relationships (SAR) and the *in vitro* effects of a focused chemical library of small molecules, possessing several key requirements for a successful inhibition of 15-LOX-1, are here described. The synthetic approach, combined to an extensive enzymatic screening supported by modeling studies, allowed the evaluation of the effects exerted by certain structural elements. Especially, the key role of non-covalent warhead groups, like phosphate and glycine moiety, as well as their positioning, and the importance of stereochemistry, has been highlighted.

Results and Discussion

Exploring Previously Identified Chiral 15-LOX-1 Inhibitors

Many 15-LOX inhibitors have been identified till now, demonstrating from moderate to good inhibitory potency. Based on the chemical structure, the majority of these inhibitors are heterocyclic small molecules, such as purine, indole, imidazole, thiophene and other scaffolds. Common feature in the above described inhibitors is their aromatic nature, while few of them present a chiral component. In order to evaluate the role of chirality in binding efficiency and, therefore, inhibition potency, we developed a database with all the reported compounds capable of inhibiting the 15-LOX-1 enzyme (inhibitory potency $<100\ \mu M$) that contained at least one chiral center. Our database includes more than 1600 compounds, which we categorized based on structure similarity and activity cliff analysis, developing the corresponding Structure-Activity Landscape Index (SALI) plot (Figure 2A). The SALI plot demonstrates how much activity is gained (or lost) with a relatively small change in structure. The generated similarity view encodes SALI values and activities in marker size and color, respectively. The cheminformatic analysis was performed in Data Warrior.

Various scaffolds can be observed in different clusters, and as expected, many of the compounds gain or lose inhibitory activity according to their different substitution pattern. However, in certain cases, a specific 3D arrangement (configuration) of the molecule has been shown to be crucial for a successful inhibition (Figure 2A). Examining their structures, we observed that they are extended lipophilic compounds that incorporate an aliphatic carbon chain with at least one chiral substituent. Moreover, all the compounds present a non-covalent warhead to bind as an anchor to the enzyme's pocket, such as salicylate, catechol, phosphate group and N-glycine. Through SAR analysis, we revealed some important findings; we believe that the binding position of the warhead plays a crucial role as it delimits its extended aliphatic chain that mimics the enzyme's natural substrates binding on the lipophilic pocket. Noteworthy examples are the inhibitors **1a,b** (Eleftheriadis-14d/e), **2a,b** and **3** (Nordihydroguaiaretic acid, NDGA), **4a,b** and **5a,b** (Figure 2A). The NDGA belongs to the lignans natural compounds class; its inhibitory effect is reported to derive from the free phenolic hydroxyl functional groups (catechol).[45] Also, these derivatives share the same aliphatic linker tale carrying two stereogenic centers, identified as one pure diastereomer. It seems that all the derivatives bind with the same direction and binding pose, interacting with specific site of the pocket. On the other hand, the more active compounds **1a** and **2b**, which present the same aliphatic chain with one stereogenic center, are different enantiomers (*S* and *R* respectively). This could be explained from the proposed docking poses of the compounds, while the bind in the opposite direction in the active site of 15-LOX-1 (Figure S3).[35] The compounds **4a,b** with *R* or *S* glycine warhead presented a favorable binding for *R* enantiomer, yielding a 5-fold difference in inhibitory potency. Having the same warhead with the N-arachidonyl glycine, compound **4b** binds to the iron of 15-LOX-1 in a more favorable orientation. Finally, compounds **5a,b** are both *S* enantiomers, presenting some other important elements, such as the extended aliphatic tale and the phosphate group. We believe that these compounds anchor from the phosphate group to the entrance of the pocket, mimicking the **ZPE** phospholipid, which have been co-crystallized in the bacterial LOX (PDB: 4G33).

Based on the analysis above, we planned to use the marine natural product phosphoeleganin (**PE**, Figure 2B), a phosphorylated polyketide that we have previously isolated from the Mediterranean ascidian *Sidnyum elegans*,[46,47] to study the 15-LOX-1 catalytic site. PE has already been successfully used in a medicinal chemistry campaign for the discovery of antidiabetic lead candidates in which it was identified as a dual-type inhibitor of PTP1B and AR enzymes, emerging targets for Type 2 Diabetes Mellitus (T2DM) drug discovery.[48] In the present study, the choice to use PE as a chemical "smart" tool to investigate 15-LOX-1 active site was motivated by the fact that we recognized in this molecule, in addition to a good degree of 3D shape resembling that of the natural substrates of 15-LOX-1, all the evidenced structural elements for an effective enzyme binding (Figure 2B). In fact, **PE** acyclic framework incorporates an extended aliphatic chain including a portion highly functionalized with hydroxyls and a phosphate group, five asymmetric carbons, a non-substituted aliphatic segment, and a glycine moiety, structural traits that are also found in some metabolic derivatives of the enzyme's substrates. We hypothesized, indeed, that **PE** anchors to iron from its glycine warhead (similar with N-arachidonyl glycine), while its extended aliphatic tale occupies the lipophilic pocket. In order to aquire initial SAR information, the PE degradation products **PE-A** and **PE-B** were investigated. Moreover, through a FBLD approach, we created a small library of PE-based synthetic fragments combining several key requirements for a successful enzyme inhibition to explore the 15-LOX-1 inhibiting PE chemical space more easily.

Re-isolation of PE from *S. elegans* and its Oxidative Cleavage to Compounds PE-A and PE-B

PE was re-isolated applying our previously reported protocol based on an exhaustive extraction of samples of the tunicate *S. elegans* collected in the Bay of Pozzuoli, and application of sequential chromatographic separations and purifications of the obtained extract.[46,48] An aliquot of the isolated polyketide was

subjected to an oxidative cleavage affording **PE-A** and **PE-B** (Scheme 1A). The purity of all compounds was assured by NMR analysis, while their identity was unequivocally established by comparing their spectroscopic data with our previously reported literature.[46]

Synthesis of Compounds T1 and T2, AT1 and AT2, and AF1–4

According to the FBLD strategy, the C5-C10 segment of **PE** guided the rational design of further PE-inspired fragments including compounds **T1** and **T2, AT1** and **AT2**, and **AF1–4** (Scheme 1B). All these compounds have been prepared through a sequence of efficient, inexpensive, and straightforward reactions, according to our previously reported synthetic protocol.[49] In detail, the starting material for preparation of the tested library are the two enantiomerically pure compounds (5*S*, 8*S*, 9*R*)-tetradecan-5,8,9-triol (**T1**) and (5*S*, 8*R*, 9*S*)-tetradecan-5,8,9-triol (**T2**). Their stereochemical identity was grounded on the application of Riguera's method which analyses the $\Delta\delta_H$ sign distribution of the substituents on the asymmetric carbons of the substrate.[50–52] Indeed, compounds **T1** and **T2** have been previously prepared as model compounds in order to assign the absolute configuration at C11-C12 diol system of **PE** in a specifically designed approach to solve its stereostructure assignment.[47] Indeed, due to the flexible acyclic scaffold of **PE** with five chirality centers, this task required combination of spectroscopic analysis, organic synthesis, chiral derivatization, and database of spectroscopic information.[47,53] Therefore, in our previous work we obtained compounds **T1** and **T2** in good amount and in enantiomerically pure form starting from the commercial available *cis*-4-decenal (Figure S4). The aldehyde function was converted to (*Z*)-tetradec-8-en-5-ol as racemate by treatment with n-butyllithium; then, four stereoisomers of the tetradecane-5,8,9-triol were prepared by reaction with catalytic OsO_4 affording two diastereomeric mixtures as racemates after RP-HPLC. These mixtures were separately converted into the tris-(*R*)-MPA esters, and the chemical shift differences ($\Delta\delta_H$) calculated. The analysis of the patterns in the $\Delta\delta_H$ sign distribution, according the Riguera's models allowed to assign the absolute configuration of each triester that, after hydrolysis with a methanolic solution of NaOH, afforded the enantiomerically pure triols **T1** and **T2** (Figure S4).

Subsequently, compounds **T1** and **T2** were treated with 2,2-dimethoxypropane and a catalytic amount of *p*-toluenesulfonic acid to afford the corresponding acetonide derivatives **12** and **13** which were then converted in the corresponding 5-acetylated acetonides **14** and **15** by treatment with acetic anhydride in pyridine. The acetylated diols **AT1** and **AT2** were obtained after acidic hydrolysis at room temperature of **14** and **15** and, then subjected to the phosphorylation reaction. This last step allows to generate both phosphate regioisomers for each enantiopure acetylated compounds, enriching the structural diversity of our small library. A meticulous separation by reversed phase HPLC yielded regioisomers **AF1-AF2** and **AF3-AF4**.

Preliminary Inhibitory Evaluation of PE Against Human 15-LOX-1

We initially performed a first evaluation of **PE** against human 15-LOX-1. Moreover, in this preliminary screening we included also compounds **PE-A**, **PE-B** and **T1**, containing the **PE** main structural elements (Figure 3A) in order to explore if they are responsible for any inhibitory potency. **PE-A** and **PE-B** include the glycine and the phosphate warhead respectively, while both contain the chiral substituted aliphatic chain. On the other

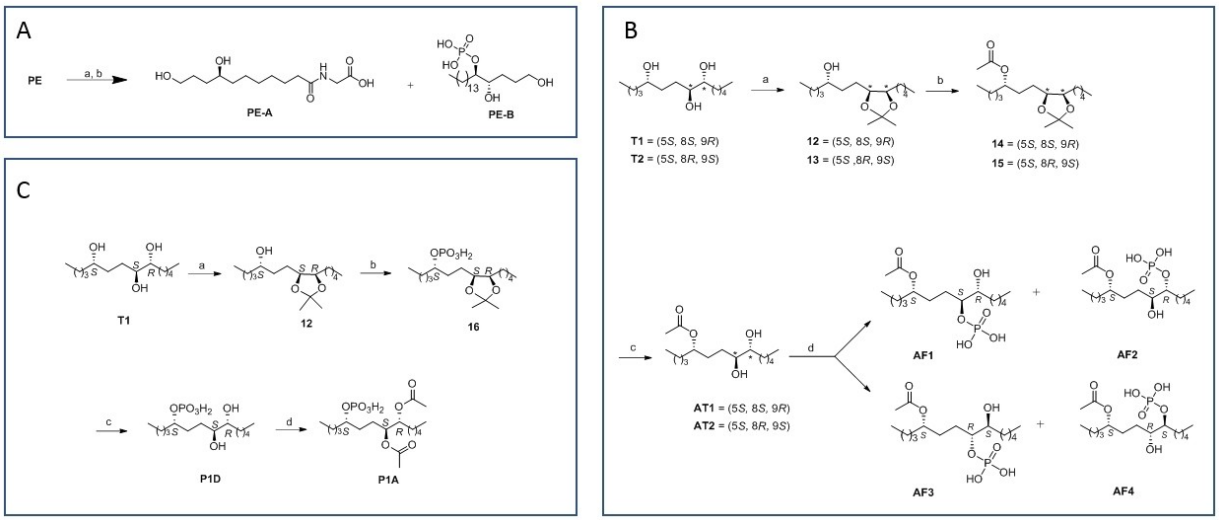

Scheme 1. A) Oxidative cleavage of PE. Reagents and conditions: (a) $NaIO_4$, MeOH, rt, 3 h. (b) $NaBH_4$, 0 °C, 1.5 h. B) Synthesis of the fragments inspired to the most functionalized portion of PE. Reagents and conditions: (a) 2,2-dimethoxypropane, *p*-toluenesulfonic acid, rt, overnight. (b) Ac_2O, pyridine, rt, overnight. (c) HCl 1%, MeOH/H_2O 9:1, rt, overnight. (d) (1) Cl_3CCN; (2) $(n\text{-}Bu)_4NH_2PO_4$, CH_3CN, rt, 2 h. C) Synthesis of the phosphorylated compounds **P1D** and **P1 A**. Reagents and conditions: (a) 2,2-dimethoxypropane, *p*-toluenesulfonic acid, r.t. overnight. (b) (1) Cl_3CCN; (2) $(n\text{-}Bu)_4NH_2PO_4$, CH_3CN, r.t. overnight. (c) (1) HCl 1%, MeOH/H_2O 9:1, r.t. overnight; (d) Ac_2O, pyridine, r.t.18 h.

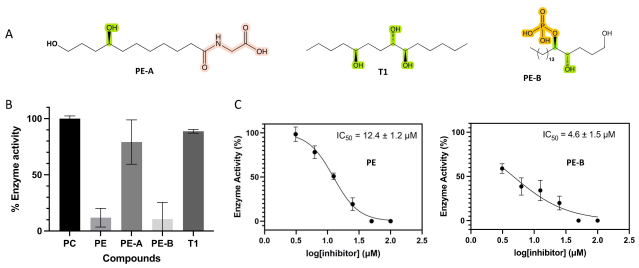

Figure 3. A) The structure of the derivatives PE–A, T1 and PE–B. B) Residual enzyme activity that was observed for the screening of a compounds collection for inhibition of h-15-LOX-1 in presence of 50 μM of the respective compounds. The enzyme activity in absence of inhibitor was set to 100% and the background signal in absence of the overexpressed h-15-LOX-1 was set to 0%. The averages and standard deviations of the individual measurements are shown. C) IC_{50} plots of h-15-LOX-1 inhibition with PE and PE–B. The results are averages of triplicates and the curves are derived by non-linear curve fitting. All the values are reported with the standard deviation after non-linear curve fitting.

hand, **T1** only presents the chiral hydroxyl substituted aliphatic chain. The 15-LOX-1 activity studies were performed using our established UV absorbance assay in a 96-well format, following the enzymatic product (234 nm) after its conversion from linoleic acid.[34,35,54–56] **PE** and **PE-B** were identified as active, providing more than 70% inhibition of the enzyme activity at concentrations of 50 μM (Figure 3B). The inhibitory potency of these compounds, confirmed by determination of their IC_{50} values, proved to be 12.4 ± 1.2 μM and 4.6 ± 1.5 μM for **PE** and **PE-B** respectively (Figure 3C). The compounds **PE-A** and **T1** demonstrated only a 20–30% inhibition at concentrations of 50 μM (Figure 3B).

These initial findings are in line with our previous analysis, that recognized in **PE** framework many key elements for enzyme inhibition. Furthermore, the phosphate warhead, lacking in the less active **PE-A** (having only the glycine warhead) or **T1** (missing both warheads), was proved to be the most critical function for the enzyme binding. Therefore, we can speculate that the different compounds warheads anchor in the opposite positions of the enzyme's pocket and that only **PE-B** yields favorable binding of the specific chiral substituents.

In order to investigate further and in more details all the above, as well as to explore the effect of the chiral substitution pattern on the inhibitory potency, we funneled into the screening against human 15-LOX-1 the remaining PE-fragments **T2**, **AT1–2**, and **AF1–4** (Scheme 1B and Figure S2). In addition, given the results of our preliminary screening, we enlarged the previously created chemical library with other phosphorylated compounds. We designed and synthesized indeed new fragments in which the phosphate group was shifted along the alkyl chain from the diol system to the isolated hydroxyl group maintaining the *5S,8S,9R* stereochemistry resembling the segment C5-C10 of the parent compound **PE**.

Enlarging the Pool of Phosphorylated Compounds: Synthesis of P1D and P1 A

To evaluate the influence of the position of the phosphate group along the tetradecan-5,8,9-triol scaffold endowed with the favorable *5S,8S,9R* stereochemistry we synthesized the new fragments **P1D** and **P1 A** slightly modifying the previously developed synthetic procedure (Scheme 1B) by changing the reactions sequence to effectively perform the phosphorylation of C5 (Scheme 1C). The update pathway involves the synthesis of acetonide as the protecting group at C8-C9, followed by the introduction of the phosphate group through the one-pot method proposed by Lira et al. as previously described[57] and, lastly, the acetylation of the diol system. This easy-to-perform method prevents the formation of pyrophosphates byproducts and requires commercially accessible reagents: tetrabutylammonium dihydrogen phosphate ($(n\text{-}Bu)_4NH_2PO4$) and trichloroacetonitrile. Interestingly, when the phosphorylation reaction was performed on compound **12** with respect to compound **AT1** the yield of phosphate monoester was greatly increased probably due to the increased solubility of **12** in acetonitrile. In detail, (*5S,8S,9R*)-tetradecan-5,8,9-triol (**T1**) was firstly treated with 2,2-dimethoxypropane and a catalytic amount of *p*-toluenesolfonic acid as to gain compound **12** in pure form and quantitative yield. Then, the acetonide derivative **12** was dissolved in acetonitrile (CH_3CN) and treated with trichloroacetonitrile, followed by dropwise addition of a CH_3CN solution of $(n\text{-}Bu)_4NH_2PO_4$. The reaction was kept under magnetic stirring at room temperature for 16 h and, after the solvent removal *in vacuo*, compound **16** was obtained. This latter was directly hydrolyzed in acidic conditions (HCl 1%) leaving mixture at 4 °C for 36 h before removing the solvent by rotary evaporator. The raw material was purified by RP-HPLC providing the phosphorylated product **P1D** in pure form as a colorless oil. Finally, a portion of the phosphorylated **P1D** was dissolved in pyridine and treated with an excess of acetic anhydride. The reaction mixture was firstly stirred for 18 h at rt, then cooled at 0 °C in an ice-bath adding MeOH to the mixture. The solvent removal in vacuo afforded the raw material which was purified by RP-HPLC yielding.

Structure-Based Analysis for Suitable Chiral Substitution Pattern

The whole chemical library of key fragments, including the newly designed compounds, was screened against 15-LOX-1 at the same concentration as the initial screening (Figure 4A), allowing identification of the active synthetic compounds **AF1** and **AF2**. Their inhibitory potency was accurately calculated (Figure 4B), showing that they are potent inhibitors of 15-LOX-1, more active than the more complex natural **PE** molecule. This primary analysis also allowed us to draw important conclusions about the importance of the stereochemistry and regiochemistry of the phosphate group in the active fragments, as described below.

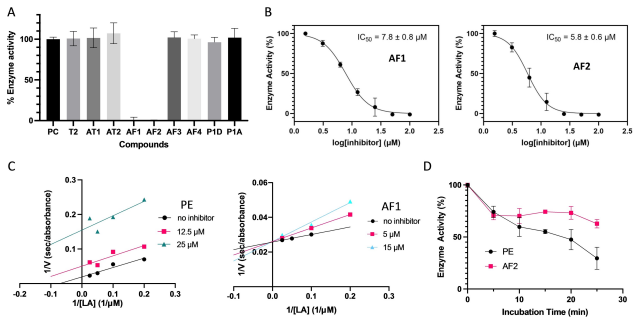

Figure 4. A) Residual enzyme activity that was observed for the screening of a compounds collection for inhibition of h-15-LOX-1 in presence of 50 μM of the respective compounds. B) IC_{50} plots of h-15-LOX-1 inhibition with AF1 and AF2. The results are averages of triplicates and the curves are derived by non-linear curve fitting. All the values are reported with the standard deviation after non-linear curve fitting. C) Steady-state kinetic characterization of h-15-LOX-1 in the presence of different concentrations of the compounds PE and AF1 with Lineweaver – Burk representation. D) A time-dependent inhibition assay in presence of the compounds PE and AF2. Five preincubation times of the respective inhibitor with the enzyme were chosen for the measurement of the time-dependent inhibition of 15-LOX-1 activity.

The importance of the phosphorylated diol system with a proper stereochemistry. Comparing **AF1** (IC_{50} = 7.8 ± 0.8 μM), with **T1** and **AT1** (both with an IC_{50} > 100 μM) is clearly evident that the presence of the phosphate group is crucial. In order to evaluate the importance of the diol stereochemistry pattern, **AF1**, designed with the same diol configuration of **PE-B** and exhibiting almost the same inhibitory potency of this semi-synthetic fragment, has been compared to **AF3**. Noteworthy, changing the diol system absolute stereochemistry of the fragment, from *S,S,R* (**AF1**) to *S,R,S* (**AF3**), leads to a completely inactive compound. Also, by shifting the phosphate group to the other hydroxyl group of the diol system, activity is maintained as long as the stereochemical pattern is unchanged. In fact, compound **AF2** (IC_{50} = 5.8 ± 0.6 μM) with the same *S,S,R* stereochemistry is active to the same extent as its regioisomer **AF1**, while its diastereoisomer **AF4**, featuring the *S,R,S* stereochemistry, is completely inactive (Figure 4A).

Only the favorable S,S,R stereochemistry is not enough. In contrast, shifting the phosphate group further to the chain on the C-5 carbon (**P1D**, **P1 A**), and even having the favorable *S,S,R* stereochemistry, activity is completely lost (Figure 4). Besides, the triols **T1** and **T2**, as well as the C-5 acetylated derivatives **AT1** and **AT2**, presenting either the *S,S,R* or the *S,R,S* stereochemistry but missing the phosphate group, are completely inactive, too.

Ultimately, through this rapid and "smart" screening of small fragments inspired to a natural hit, we have identified a chiral substitution pattern suitable for successful binding to the 15-LOX-1 pocket. Overall, our results demonstrate that phosphate group binding is dominant, driving the chiral aliphatic chain toward a favorable or not binding. In addition to having used the fragments library as chemical tool to generate new knowledge about the chiral pocket of the enzyme, we have identified in compounds **AF1** and **AF2** new inhibiting 15-LOX-1 leads for early drug discovery processes. It is noteworthy that, unlike the complex natural molecule **PE**, these compounds can be readily obtained through a feasible synthetic procedure that can be achieved with good yield, sustainable strategies, and high atomic economy.

Enzyme Kinetic Analysis

In order to investigate the binding mechanism of our compounds, we performed Michaelis-Menten enzyme kinetics analysis in presence of **AF1** and **PE** compounds. As expected, **AF1** compound revealed a competitive inhibition, as the Lineweaver-Burk plot shows that the inhibitor causes an increase in the K_M values, whereas the V_{max} values remain constant (Figure 4C, Table S1). However, PE caused a decrease in both the K_M and V_{max} values (Figure 4C, Table S2), indicating an uncompetitive inhibition mechanism of 15-LOX-1. These findings expose the involvement of the glycine warhead in the chelation on the iron in the active site of 15-LOX-1. We confirmed our hypothesis, performing a time-dependent inhibition assay in presence of **PE** and **AF2** (Figure 4D). In this experiment, the enzyme was incubated with the inhibitors for various time frames from 5 to 25 min, and then the remaining enzyme activity was measured. We observed than only in case of **PE**, we had a time-dependent inhibition, caused by increased binding and chelation of iron followed by enzyme inactivation. We believe that, for such compounds as **4 a,b**, the mechanism of PE binding is similar to N-arachidonyl glycine, which is a metabolite that contains a glycine warhead group with known chelating properties.[58–60] Instead, compounds **AF1** and **AF2**, having only the phosphate group, bind to the enzyme's active site and its tale occupies the lipophilic pocket, similarly to compounds **5 a,b**.

Molecular Modelling

To justify our results and propose possible binding poses of our compounds, we performed molecular modeling studies. Through that, we were able to explore unknown enzyme's pocket potentials related to chiral binding. In order to link the observed inhibitory potency and kinetic analysis to structural information, selected compounds were docked in the active site of the enzyme. Since there in no available crystal structure of human 15-LOX-1, rabbit 15-LOX was used in the molecular modeling studies, as determined by Gillmor et al.[33] The molecular modeling studies were performed in MOE software and highest scoring docking poses were chosen. The experiments were performed with rescoring model 1 London dG (refinement: forcefield) and rescoring 2: GBVI/WSA dG, followed by minimization energy (forcefield: MMFF94X; eps 1/4 r, cutoff {8,10}). The best inhibitory potency of **PE-B** is reflected in its highest docking score compared to the other investigated compounds with weak or no inhibition for h-15-LOX-1 (Table 1). The top three highest scoring poses enabled the proposal of a binding configuration in which **PE-B** anchors with its phosphate group in the polar entrance of the pocket, forming a hydrogen

Table 1. Comparison of h-15-LOX-1 inhibition values with docking scores in the enzyme's active site.

Compounds	Docking Score	IC_{50} value (μM)
PE-B	−10.45	4.6 ± 1.5
AF1	−9.01	7.8 ± 0.8
AF4	−8.43	> 100
AT1	−8.24	> 100
T1	−7.71	> 100
PE	1.93	12.4 ± 1.2

bond with the **Arg403**, while its aliphatic chain occupies the hydrophobic active site with lipophilic interactions (Figure 5A). This proposed binding pose is in line with the co-crystal structure of **ZPE** phospholipid in the bacterial PA-LOX. To verify that, we performed alignment of the two protein structures, which revealed a high structural similarity and the **ZPE** binds with the same orientation in the active site of both enzyme (Figure S5). Moreover, in line with the enzyme kinetic analysis, the competitive inhibitor **AF1** binds to the enzyme's pocket with high docking score. The proposed pose revealed an involvement of the phosphate in an interaction with iron in the enzyme. However, this interaction cannot be observed in the binding poses of the inactive compounds **AF4**, **T1** and **AT1**, yielding lower docking scores. Importantly, we observed an opposite binding orientation of these compounds compare to **AF1**, something that could explain their poor inhibitory potency. It seems that in case of **AF4**, the unfavorable *S,R,S* stereochemistry is responsible for that (Figure 5B), while for **T1** and **AT1**, the absence of the phosphate group is the major factor, irrespectively of the correct *S,S,R* stereochemistry (Figure 5C and D). Finally, when we tried to dock the **PE** compound in the active site of the enzyme, an unfavorable score was calculated, mainly coming from steric hindrances (Figure S6). These findings enhanced our hypothesis that **PE** inactivates the enzyme over time through the chelation of the iron from its glycine warhead.

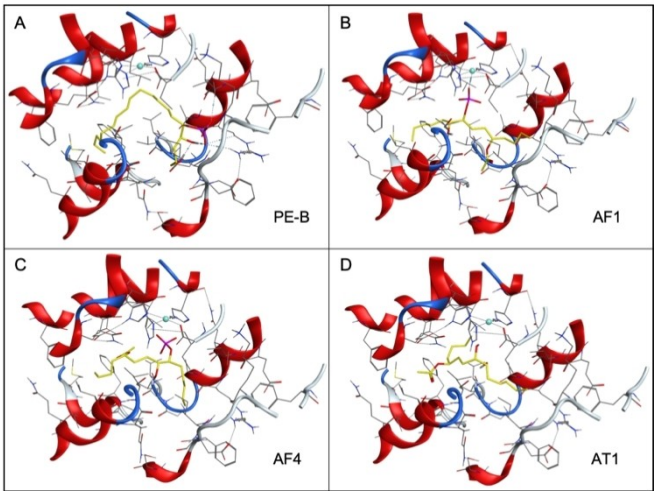

Figure 5. Binding of compound A) **PE-B**, B) **AF1**, C) **AF4** and D) **AT1** in the active site of 15-LOX-1 after molecular modeling studies.

Conclusions

In this study, we highlighted the importance of critical structural elements, such as a proper chirality in combination with the positioning of phosphate and glycine anchor groups, in the inhibitors for the enzyme human 15-LOX-1. To this purpose, we utilized the marine derived natural hit **PE** among with a synthetic fragments small library inspired by the natural molecule and including certain degree of stereochemical diversity. These fragments were used as "smart" tools against the human 15-LOX-1 to reveal unexplored features of enzyme's active site. Enzyme inhibition and kinetic studies, as well as molecular modelling studies has been performed in order to characterize structurally novel PE-based inhibitors, which proved to present a different type of inhibition, according to their structural features. We demonstrate that the phosphate warhead, present in the semisynthetic derivative **PE-B**, works as anchor and guides specific stereochemistry, as it can strongly bind to the polar entrance and specifically with **Arg403**. Moreover, we reveal that compounds containing a glycine warhead, such as **PE** and **PE-A** in line with previously identified **4a,b** and N-arachidonyl glycine, can chelate the iron of the enzyme over time, causing a time-depended inhibition. Finally, we prove that just the positioning of the substituents on the chiral centers, and thus, a favorable stereochemistry can be crucial, as it can lead from active (**AF1, AF2**) to completely inactive compounds (**AF3, AF4**). In the future, the acquired knowledge as well as the **PE** derivatives and/or inspired compounds could be employed for drug discovery efforts in selective targeting of h-15-LOX-1.

Experimental Section

General methods: 1D and 2D NMR spectra were recorded on Bruker Avance Neo spectrometer (Bruker BioSpin Corporation, Billerica, MA, USA); Coupling constants (J values) are given in Hertz (Hz), chemical shifts are reported in ppm and referred to the residual solvent signal (CD_3OD: $\delta_H = 3.31$, $\delta_C = 49.0$; $CDCl_3$: $\delta_H = 7.26$, $\delta_C = 77.0$;). All the recorded signals are in accordance with the proposed structures. Spin multiplicities are given as s (singlet), br s (broad singlet), d (doublet), dd (doublet of doublets), t (triplet), br t (broad triplet) or m (multiplet). When the multiplicity could not be recognized because of merged signals, overlapped was used. High-resolution MS (both positive and negative mode) was performed on a Thermo LTQ Orbitrap XL mass spectrometer (Thermo-Fisher, San Josè, CA, USA). The MS spectra of all compounds and intermediates were recorded by infusion into the ESI source using MeOH as solvent. High performance liquid chromatography (HPLC) separation was achieved on a Knauer K-501 apparatus equipped with a Knauer K-2301 RI detector (LabService Analytica s.r.l., Anzola dell'Emilia, Italy). Solvents and reagents were purchased from commercial sources (Sigma-Aldrich-Merck) and used without any purifications except of (5*S*,8*S*,9*R*)-tetradecan-5,8,9-triol (**T1**) and (5*S*,8*R*,9*S*)-tetradecan-5,8,9-triol (**T2**) which were synthesized according to the reported method.[47] Reaction progress was monitored

via thin layer chromatography (TLC) on Silica Gel 60 F254, plates 5×20, 0.25 mm.

*Extraction and Isolation of phoshoeleganin (**PE**) from S. elegans:* Specimens of *S. elegans* collected at Pozzuoli (Naples, Italy, April 2019) were available in Department of Pharmacy, University of Naples Federico II. They were frozen immediately after collection and kept frozen until extraction. A fresh thawed sample (23.1 g of dry weight after extraction) were extracted according to a previously reported procedure.[46] The butanol soluble material was chromatographed by MPLC over a C18 column following a gradient elution $H_2O \rightarrow MeOH \rightarrow CHCl_3$. The fraction eluted with $MeOH/H_2O$ 7:3 (v/v) was further purified by HPLC on reversed phase (Synergi RP-MAX 4 μm 250 mm×4.6 mm column, $MeOH/H_2O$ 8:2 + 0.1% TFA) and afforded **PE** ($t_R = 20.5$ min, 17.2 mg) in pure form. PE: colourless oil; ESIMS: $[M-H]^-$ *m/z* 668.65. All data agree with those reported in the literature.[46]

Enzyme Activity assay: The h-15-LOX-1 was expressed in BL21 (DE3) *E. coli* cells and the cell lysate was used for the activity assay with no further purification. The conversion of linoleic acid to 13S-hydroperoxy-9Z,11E-octadecadienoic acid (13(S)-HpODE) was observed through UV absorbance at 234 nm over time with a ThermoFisher Varioskan Plate Reader and a Greiner Bio-One F-Bottom 96-well plate. The measurement took place for 20 min with an interval time of 20 sec. Only the linear part was used for the determination of the enzymatic activity, typically extending over the first 1–5 min depending on the enzyme concentration. After that, the conversion rate slows down due to the consumption of the substrate. The activity assay was used for the determination of the optimum concentration of the cell lysate (×200 times dilution in assay buffer: 50 mM HEPES, 50 mM NaCl, pH 7,5). Linoleic acid (Sigma Aldrich, L1376) was diluted in ethanol. Each measurement was performed in triplicate and all data were processed with Microsoft Excel Professional Plus 2016 and GraphPad Prism 8 software.

Enzyme inhibition assay: For the evaluation of the inhibitory potency of the compounds the same experimental approach based on the absorption of 13(S)-HpODE at 234 nm was used. All the compounds were dissolved in DMSO at a final concentration of 2 mM. Then, they were diluted with assay buffer and tested at 50 μM. Each compound was mixed with the diluted cell lysate and after a 10 minute incubation at RT, the linoleic acid was added at a final concentration of 25 μM. All the values were normalized by setting as 100% the absence of the inhibitor. Compounds in test samples with enzyme activity less than 50% were considered as hits. Each measurement was performed in triplicate and all data were processed with Microsoft Excel Professional Plus 2016 and GraphPad Prism 8 software.

Determination of the half maximal inhibitor concentration (IC_{50}): The half maximal inhibitor concentration (IC_{50}) was also determined by a comparable method using the absorption of 13(S)-HpODE at 234 nm. All the compounds were firstly dissolved in DMSO and then diluted with assay buffer at a final concentration of 200 μM. The desired concentrations, ranging from 0,78 to 100 μM, were achieved by serial dilution. Each concentration was mixed with the diluted cell lysate and after a 10 minute incubation at RT, the linoleic acid was added at the same final concentration as above. The 100% was set by the absence of the inhibitor, while the 0% was set by the absence of the substrate. DMSO, diluted in assay buffer, was added to both the positive control and the blank sample at the same concentration as the test sample. Each measurement was performed in triplicate and all data were processed with Microsoft Excel Professional Plus 2016 and GraphPad Prism 8 software.

Michaelis–Menten kinetics: The absorption of 13(S)-HpODE at 234 nm was employed once again for the kinetics study. Four different concentrations of the linoleic acid were tested this time: 5 μM, 10 μM, 20 μM and 40 μM. The enzyme activity was determined in the absence or presence of specified concentrations of the inhibitors based on their IC_{50} value. As previously, 100 μl of the inhibitor solution were mixed with 40 μl of assay buffer and 50 μl of the diluted cell lysate. In absence of inhibitor, the corresponding volume is replaced with assay buffer. After a 10 minute incubation at RT, 10 μl of linoleic acid ranging from 800 μM to 100 μM. The reaction velocity V was plotted against the substrate concentration [S] in a Michaelis – Menten plot for the determination of the K_m and V_{max} in the presence of the inhibitor. The reciprocal of the substrate concentration 1/[S] was plotted against the reciprocal of the reaction velocity 1/V in a Lineweaver Burk plot. Each measurement was performed in triplicate and all data were processed with Microsoft Excel Professional Plus 2016 and GraphPad Prism 8 software.

Supporting Information Summary

The authors have cited additional references within the Supporting Information.

Acknowledgements

We acknowledge a) the Empeirikeion Foundation, b) the National Recovery and Resilience Plan Greece 2.0, funded by the European Union–NextGenerationEU (project code: TAEDR-0535850) and c) the Hellenic Foundation for Research and Innovation (H.F.R.I.) under the Greece 2.0 Basic Research Financing Action «Horizontal support of all sciences» Sub-action 2 (project number: 15511) for providing grants to N.E. We acknowledge financial support under the National Recovery and Resilience Plan (NRRP) by the Italian Ministry of University and Research (MUR) funded by the European Union–NextGenerationEU (project code: PRIN 2022 PNRR: P2022PPH4 C). We also acknowledge Prof. T. Holman (University of California, Santa Cruz) for providing the human 15-LOX-1 plasmid.

Conflict of Interests

The authors declare no conflict of interest.

Data Availability Statement

The data that support the findings of this study are available in the supplementary material of this article.

Keywords: Human 15-lipoxygenase 1 · Phosphoeleganin · Marine drugs · Fragment-based lead discovery · Inflammation

[1] J. Zhao, V. B. O'Donnell, S. Balzar, C. M. St. Croix, J. B. Trudeau, S. E. Wenzel, *Proc. Natl. Acad. Sci. U. S. A.* **2011**, *108*, 14246–14251.

[2] U. Mabalirajan, R. Rehman, T. Ahmad, S. Kumar, G. D. Leishangthem, S. Singh, A. K. Dinda, S. Biswal, A. Agrawal, B. Ghosh, *Sci. Rep.* **2013**, *3*, 1540.
[3] U. Mabalirajan, R. Rehman, T. Ahmad, S. Kumar, S. Singh, G. D. Leishangthem, J. Aich, M. Kumar, K. Khanna, V. P. Singh, et al., *Sci. Rep.* **2013**, *3*, 1349.
[4] A. R. Lindley, M. Crapster-Pregont, Y. Liu, D. A. Kuperman, *Mediators Inflamm.* **2010**, *2010*, 727305.
[5] J. Z. Haeggström, C. D. Funk, *Chem. Rev.* **2011**, *111*, 5866–5898.
[6] K. van Leyen, *CNS Neurol. Disord. - Drug Targets* **2013**, *12*, 191–199.
[7] P. F. Giannopoulos, Y. B. Joshi, J. Chu, D. Praticò, *Aging Cell* **2013**, *12*, 1082–1090.
[8] Y. B. Joshi, P. F. Giannopoulos, D. Praticò, *Trends Pharmacol. Sci.* **2015**, *36*, 181–186.
[9] D. Praticò, V. Zhukareva, Y. Yao, K. Uryu, C. D. Funk, J. a Lawson, J. Q. Trojanowski, V. M.-Y. Lee, *Am. J. Pathol.* **2004**, *164*, 1655–1662.
[10] K. van Leyen, H. Y. Kim, S.-R. Lee, G. Jin, K. Arai, E. H. Lo, *Stroke* **2006**, *37*, 3014–3018.
[11] A. Fiedorowicz, H. Car, S. Prokopiuk, E. Sacharzewska, M. Żendzian, K. Kowal, *Prog Heal. Sci* **2013**, *3*, 33–38.
[12] K. van Leyen, K. Arai, G. Jin, V. Kenyon, B. Gerstner, P. a Rosenberg, T. R. Holman, E. H. Lo, *J. Neurosci. Res.* **2008**, *86*, 904–909.
[13] S. Tobaben, J. Grohm, A. Seiler, M. Conrad, N. Plesnila, C. Culmsee, *Cell Death Differ.* **2011**, *18*, 282–292.
[14] F. Succol, D. Praticò, *J. Neurochem.* **2007**, *103*, 380–387.
[15] J. Chu, J.-G. Li, P. F. Giannopoulos, B. E. Blass, W. Childers, M. Abou-Gharbia, D. Praticò, *Mol. Psychiatry* **2015**, *20*, 1329–1338.
[16] A. J. Klil-Drori, A. Ariel, *Prostaglandins Other Lipid Mediat.* **2013**, *106*, 16–22.
[17] M. A. Vaezi, B. Safizadeh, A. R. Eghtedari, S. S. Ghorbanhosseini, M. Rastegar, V. Salimi, M. Tavakoli-Yaraki, *Lipids Health Dis.* **2021**, *20*, 169.
[18] H.-E. Claesson, W. J. Griffiths, Å. Brunnström, F. Schain, E. Andersson, S. Feltenmark, H. A. Johnson, A. Porwit, J. Sjöberg, M. Björkholm, *FEBS J.* **2008**, *275*, 4222–4234.
[19] E. Andersson, F. Schain, J. Sjöberg, M. Björkholm, H.-E. Claesson, *Exp. Hematol.* **2010**, *38*, 116–123.
[20] F. Schain, D. Schain, Y. Mahshid, C. Liu, A. Porwit, D. Xu, H.-E. Claesson, C. Sundström, M. Björkholm, J. Sjöberg, *Clin. Lymphoma Myeloma* **2008**, *8*, 340–347.
[21] Y. Chen, C. Peng, S. A. Abraham, Y. Shan, Z. Guo, N. Desouza, G. Cheloni, D. Li, T. L. Holyoake, S. Li, *J. Clin. Invest.* **2014**, *124*, 3847–3862.
[22] M. K. Middleton, A. M. Zukas, T. Rubinstein, M. Jacob, P. Zhu, L. Zhao, I. Blair, E. Puré, *J. Exp. Med.* **2006**, *203*, 2529–2540.
[23] S. V. K. Mahipal, J. Subhashini, M. C. Reddy, M. M. Reddy, K. Anilkumar, K. R. Roy, G. V. Reddy, P. Reddanna, *Biochem. Pharmacol.* **2007**, *74*, 202–214.
[24] K. A. Kumar, K. M. Arunasree, K. R. Roy, N. P. Reddy, A. Aparna, G. V. Reddy, P. Reddanna, *Biotechnol. Appl. Biochem.* **2009**, *52*, 121.
[25] B. Samuelsson, S. E. Dahlén, J. A. Lindgren, C. A. Rouzer, C. N. Serhan, *Science* **1987**, *237*, 1171–1176.
[26] E. Sigal, C. W. Laughton, M. A. Mulkins, *Ann. N. Y. Acad. Sci.* **1994**, *714*, 211–24.
[27] D. Li, Y. Li, *Signal Transduct. Target. Ther.* **2020**, *5*, 108.
[28] E. Grignano, R. Birsen, N. Chapuis, D. Bouscary, *Front. Oncol.* **2020**, *10*, 1–10.
[29] L. Probst, J. Dächert, B. Schenk, S. Fulda, *Biochem. Pharmacol.* **2017**, *140*, 41–52.
[30] W. S. Yang, K. J. Kim, M. M. Gaschler, M. Patel, M. S. Shchepinov, B. R. Stockwell *Proc. Natl. Acad. Sci.* **2016**, *113*, E4966–E4975.
[31] W. S. Yang, B. R. Stockwell, *Trends Cell Biol.* **2016**, *26*, 165–176.
[32] H. Feng, B. R. Stockwell, *PLOS Biol.* **2018**, *16*, e2006203.
[33] S. A. S. A. Gillmor, A. Villaseñor, R. Fletterick, E. Sigal, M. F. M. F. Browner, *Nat. Struct. Biol.* **1997**, *4*, 1003–1009.
[34] N. Eleftheriadis, C. G. Neochoritis, N. G. J. Leus, P. E. van der Wouden, A. Dömling, F. J. Dekker, *J. Med. Chem.* **2015**, *58*, 7850–7862.
[35] N. Eleftheriadis, S. Thee, J. te Biesebeek, P. van der Wouden, B.-J. J. Baas, F. J. Dekker, *Eur. J. Med. Chem.* **2015**, *94*, 265–275.
[36] I. P. Silvestri, P. J. J. Colbon, *ACS Med. Chem. Lett.* **2021**, *12*, 1220–1229.
[37] N. T. Tzvetkov, K. Kirilov, M. Matin, A. G. Atanasov, *Nephrol. Dial. Transplant.* **2024**, *39*, 375–378.
[38] A. G. Atanasov, S. B. Zotchev, V. M. Dirsch, C. T. Supuran, *Nat. Rev. Drug Discov.* **2021**, *20*, 200–216.
[39] M. Casertano, A. Vito, A. Aiello, C. Imperatore, M. Menna, *Pharmaceutics* **2023**, *15*, 2321.
[40] A. H. Banday, N. ul Azha, R. Farooq, S. A. Sheikh, M. A. Ganie, M. N. Parray, H. Mushtaq, I. Hameed, M. A. Lone, *Phytochem. Lett.* **2024**, *59*, 124–135.
[41] X. Fu, F. J. Schmitz, M. Govindan, S. A. Abbas, K. M. Hanson, P. A. Horton, P. Crews, M. Laney, R. C. Schatzman, *J. Nat. Prod.* **1995**, *58*, 1384–1391.
[42] R. H. Cichewicz, V. A. Kenyon, S. Whitman, N. M. Morales, J. F. Arguello, T. R. Holman, P. Crews, *J. Am. Chem. Soc.* **2004**, *126*, 14910–14920.
[43] H. Sadeghian, A. Jabbari, *Expert Opin. Ther. Pat.* **2016**, *26*, 65–88.
[44] T. Amagata, S. Whitman, T. A. Johnson, C. C. Stessman, C. P. Loo, E. Lobkovsky, J. Clardy, P. Crews, T. R. Holman, *J. Nat. Prod.* **2003**, *66*, 230–235.
[45] S. Whitman, M. Gezginci, B. N. Timmermann, T. R. Holman, *J. Med. Chem.* **2002**, *45*, 2659–2661.
[46] C. Imperatore, P. Luciano, A. Aiello, R. Vitalone, C. Irace, R. Santamaria, J. Li, Y.-W. Guo, M. Menna, *J. Nat. Prod.* **2016**, *79*, 1144–1148.
[47] P. Luciano, C. Imperatore, M. Senese, A. Aiello, M. Casertano, Y.-W. Guo, M. Menna, *J. Nat. Prod.* **2017**, *80*, 2118–2123.
[48] M. Genovese, C. Imperatore, M. Casertano, A. Aiello, F. Balestri, L. Piazza, M. Menna, A. Del Corso, P. Paoli, *Mar. Drugs* **2021**, *19*, DOI: 10.3390/md19100535.
[49] M. Casertano, M. Genovese, L. Piazza, F. Balestri, A. Del Corso, A. Vito, P. Paoli, A. Santi, C. Imperatore, M. Menna, *Pharmaceuticals* **2022**, *15*, DOI: 10.3390/ph15030325.
[50] V. Leiro, J. M. Seco, E. Quiñoá, R. Riguera, *Org. Lett.* **2008**, *10*, 2729–2732.
[51] J. M. Seco, E. Quiñoá, R. Riguera, *Chem. Rev.* **2004**, *104*, 17–118.
[52] R. Sparaco, P. Cinque, A. Scognamiglio, A. Corvino, G. Caliendo, F. Fiorino, E. Magli, E. Perissutti, V. Santagada, B. Severino, et al., *Molecules* **2024**, *29*, DOI: 10.3390/molecules29071598.
[53] T. F. Molinski, B. I. Morinaka, *Tetrahedron* **2012**, *68*, 9307–9343.
[54] N. Eleftheriadis, S. A. Thee, M. R. H. Zwinderman, N. G. J. Leus, F. J. Dekker, *Angew. Chemie - Int. Ed.* **2016**, *55*, 12300–12305.
[55] N. Eleftheriadis, H. Poelman, N. G. J. Leus, B. Honrath, C. G. Neochoritis, A. Dolga, A. Dömling, F. J. Dekker, *Eur. J. Med. Chem.* **2016**, *122*, 786–801.
[56] R. van der Vlag, H. Guo, U. Hapko, N. Eleftheriadis, L. Monjas, F. J. Dekker, A. K. H. Hirsch, *Eur. J. Med. Chem.* **2019**, *174*, 45–55.
[57] L. M. Lira, D. Vasilev, R. A. Pilli, L. A. Wessjohann, *Tetrahedron Lett.* **2013**, *54*, 1690–1692.
[58] J. J. Prusakiewicz, P. J. Kingsley, K. R. Kozak, L. J. Marnett, *Biochem. Biophys. Res. Commun.* **2002**, *296*, 612–617.
[59] N. Parmar, W. V. Ho, *Br. J. Pharmacol.* **2010**, *160*, 594–603.
[60] T. Marino, M. Toscano, N. Russo, A. Grand, *J. Phys. Chem. B* **2006**, *110*, 24666–24673.

Manuscript received: June 13, 2024
Accepted manuscript online: July 23, 2024
Version of record online: ■■, ■■

RESEARCH ARTICLE

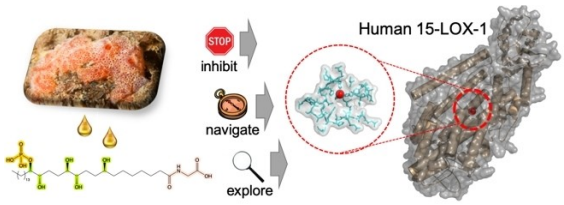

N. Spacho, M. Casertano, C. Imperatore, C. Papadopoulos, M. Menna, N. Eleftheriadis**

1 – 10

Investigating the Catalytic Site of Human 15-Lipoxygenase-1 *via* Marine Natural Products

Human 15-lipoxygenase-1 is an enzyme with a key role in various diseases. We developed a library of chiral smart molecules to explore, navigate and inhibit this enzyme, integrating specific structural elements from marine-derived natural product phosphoeleganin (PE) and synthetic fragment derivatives. These PE-based inhibitors exhibit time-dependent inhibition and varying potency based on stereochemistry and warhead positioning.